Laser-Induced Fluorescence Spectrum of 3-Vinyl-1*H*-indene

Hong-Ming Yin,† B. R. Heazlewood, N. P. J. Stamford, Klaas Nauta, G. B. Bacskay, S. H. Kable, and T. W. Schmidt*

School of Chemistry, University of Sydney, NSW 2006, Australia

Received: December 22, 2006; In Final Form: February 27, 2007

The laser-induced fluorescence spectrum of 3-vinyl-1*H*-indene was recorded between 33 000 and 33 800 cm^{-1}. An origin band was observed at 33 455 cm^{-1} along with several low-frequency modes. With the aid of density functional theory and configuration interaction calculations, the electronic transition was assigned as $S_1 \leftarrow S_0$ and the short progression in an 80 cm^{-1} mode was identified as a vinyl group torsion. Theoretical, spectroscopic, and thermochemical considerations suggest that the 3-vinyl-1*H*-indene spectrum results from excitation from both conformational isomers with the vinyl and indene double bonds in trans and cis arrangements. The results are discussed in the context of the identification of species arising from the discharge of benzene in argon.

I. Introduction

Aromatic molecules are found in the products of combustion[1−3] and discharges,[4] and are postulated to account for a large proportion of interstellar carbon.[5,6] Recent spectroscopic studies on the products of a discharge of benzene in argon have been motivated by the quest to identify carriers of the diffuse interstellar bands (DIBs), a series of unidentified absorption features seen in the spectra of lines of sight toward reddened stars.[7,8] Indeed, of the few benzene discharge products observed to absorb in the visible region, two have been found to be coincident with broad DIBs.[9−11] The spectroscopy of the benzene discharge in the midultraviolet region is complex, as this is where a myriad of medium-sized substituted benzenes absorb.[12]

The benzene/Ar discharge provides a very rich chemical environment. In addition to very small fragments, such as C_2 and C_3,[11] several larger, stable aromatic species have already been identified, including phenylacetylene, styrene, indene, tolane, fluorene, and methylstyrene.[4] However, there are even more species as yet unidentified. Two of the stronger unidentified spectra were found to correspond to masses 128 and 142,[4,13] peaks which would be tempting to ascribe to naphthalene and methylnaphthalene in the absence of firm spectroscopic identification. Subsequent work has shown that the mass 128 spectrum observed was largely due to 1-phenyl-1-buten-3-yne.[14] It is a sensible starting point to assume that the carrier of the mass 142 spectrum is also built onto an aromatic chromophore and the empirical formula $C_{11}H_{10}$ (verified by d_6-benzene discharge[13]) suggests three additional double-bond equivalents in addition to benzene. The presence of indene and styrene in the discharge[4] prompted us to suggest one of the vinylindene isomers as a potential carrier of the 142 amu spectrum. There has been no previous electronic spectroscopic investigation of any of the vinylindenes. Such a molecule is expected to exhibit a spectrum shifted to lower energy by about 6000 cm^{-1} compared to benzene, as each conjugated vinyl group shifts the $S_1 \leftarrow S_0$ spectrum about 3000 cm^{-1} to lower energy. Of the vinylindenes, the 1-vinyl-1*H*-indene is not fully conjugated. Of the others, 3-vinyl-1*H*-indene may be formed by addition of a single linear C_5 fragment to a C_6 ring, while the 2-vinyl-1*H*-indene would require addition of a branched structure, which seems less likely.

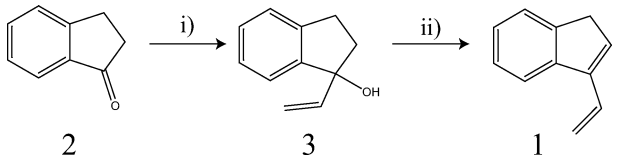

Figure 1. Synthetic route to 3-vinyl-1*H*-indene. 1-Indanone (**2**) is treated with reagent (i: CH_2═CHMgBr, in THF, Δ, 1 h) to afford 3-vinylindan-3-ol (**3**). This was dehydrated (ii: quinoline, I_2, benzene, Δ, 3 h, dark) to yield the product, 3-vinyl-1*H*-indene (**1**). Details of the synthesis are contained in the text.

The present study is motivated by our desire to identify the products and intermediates of a benzene discharge, in order to understand hydrocarbon chemistry in such environments. Here we present the laser-induced fluorescence spectrum of 3-vinyl-1*H*-indene, along with a theoretical analysis based on density functional and configuration interaction calculations. Our negative identification of 3-vinyl-1*H*-indene as the carrier of the mass 142 spectrum makes its eventual identification all the more intriguing.

II. Experimental Section

A. Synthesis of 3-Vinyl-1*H*-indene. 3-Vinyl-1*H*-indene (**1**) was synthesized by the reported method of Quin et al.[15] and Chevykalova et al.[16] starting from 1-indanone (**2**) over a two-step reaction sequence (Figure 1). Initially, 3-vinylindan-3-ol (**3**; 78% yield) was synthesized from 1-indanone (**2**) via Grignard addition with vinylmagnesium bromide in refluxing dry tetrahydrofuran. The resulting oil, which solidified upon cooling, was stored in the freezer (−30 °C) without any visible decomposition. Dehydration of the alcohol **3** was performed in refluxing benzene with a Dean−Stark apparatus. The reaction

* To whom correspondence should be addressed. E-mail: t.schmidt@chem.usyd.edu.au.

† Present address: State Key Laboratory of Molecular Reaction Dynamics, Dalian Institute of Chemical Physics, CAS, Dalian, 116023, China.

10.1021/jp068844d CCC: $37.00
Published on Web 04/11/2007

was kept in the dark under a stream of dry nitrogen to curtail polymerization of the developing 3-vinyl-1*H*-indene (**1**). Purification by flash chromatography gave the desired 3-vinyl-1*H*-indene (**1**) in 58% yield as a pale yellow oil with a faint benzene-like odor. This material was kept in the dark and stored under a dry atmosphere of nitrogen in the freezer (−30 °C). After 3 days this compound was assessed for decomposition and/or polymerization through a process of re-purification. Upon the addition of hexane a white solid was seen to precipitate, which was not further analyzed. The soluble material was again purified by flash chromatography to afford the desired 3-vinyl-1*H*-indene (**1**) in 35% yield from the previously isolated material. Additional preparations were utilized directly following purification by flash chromatography. NMR spectra revealed the fresh samples to be pure.

B. Laser-Induced Fluorescence Spectroscopy. The laser-induced fluorescence (LIF) apparatus has been described in detail elsewhere.[17] Jet-cooled 3-vinyl-1*H*-indene (vinylindene) was produced by a supersonic expansion of argon. Vinylindene was entrained in the carrier gas by passing it through a heated sample reservoir and nozzle assembly (≈80 °C). Typical operating pressure throughout the experiment was 1×10^{-4} Torr with a stagnation pressure of 3 bar behind the nozzle.

Medium-resolution LIF excitation spectra were obtained by interrogating the molecular beam approximately 30 mm downstream of the nozzle with an Nd:YAG pumped tunable dye laser. The fluorescence was imaged by a quartz lens (*f*/1.5) into a monochromator mounted to the vacuum chamber at 135° to the laser beam. The monochromator was equipped with 5 mm entry and exit slits, corresponding to a 20 nm bandpass at FWHM, to minimize scattered laser light. The imaged light was detected by a photomultiplier tube mounted at the monochromator exit. The signal from the photomultiplier was preamplified and integrated with a gated boxcar averager. The digitized output was recorded on a personal computer. An oscilloscope was used to view the fluorescence decay profile. Relative instrument timings were controlled by a digital delay generator operated at a repetition rate of 10 Hz. Absolute frequency calibration of the pump laser was obtained with a wavemeter.

As the sample was found to decay to 35% within 3 days, even when held at −30 °C, we may assume that its survival in the heated sample reservoir was much shorter. Indeed, the fluorescence signal was often difficult to find, which we attribute to the sample decaying within the time required to optimize our apparatus. The decayed sample resembled a resinous material that we assumed to be polyvinylindene.

No fluorescence signal was found in the region of the unidentified mass 142 band near 32 000 cm^{-1}. As such, the excitation laser was scanned to higher energies until fluorescence signal was located at 33 455 cm^{-1}.

III. LIF Spectrum

The LIF spectrum is depicted in Figure 2. There is a clear origin band at 33 455 cm^{-1} with a short progression in a low-frequency mode of about 80 cm^{-1}. This progression also appears to be built onto numerous other bands. At higher energy another low-frequency progression with a frequency of about 60 cm^{-1} seems evident, although the higher density of transitions makes this assignment more speculative.

We scanned about 500 cm^{-1} further to lower energy than shown in Figure 2. Some very weak features were observed, which we attribute to hot bands. Due to difficulties associated with sample preparation and handling, we were unable to extend our study to higher energies.

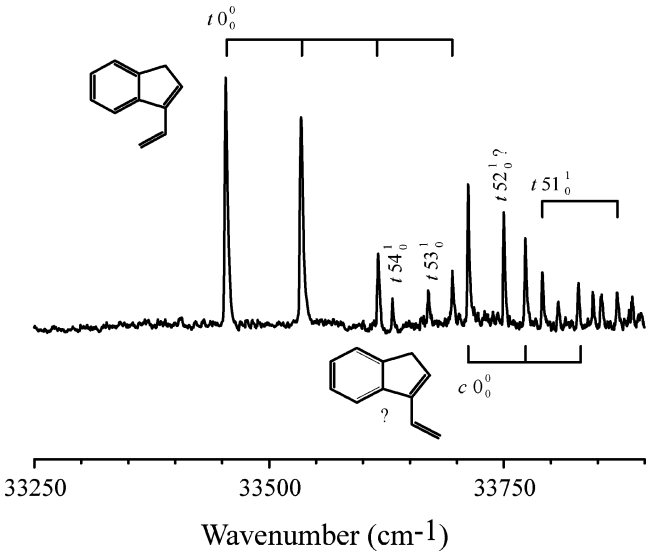

Figure 2. LIF spectrum of vinylindene. Assignment and structure for the trans conformer are shown above the spectrum, whereas more tentative assignments for the cis conformer are shown below. Progressions as indicated are for torsional motion in ν_{57}.

Vinylindene has 57 degrees of vibrational freedom. Assignment of the LIF spectrum, even in this low-frequency regime, can only be achieved with the assistance of theoretical calculations.

IV. Theory

The torsional mode of the vinyl group in vinylindene affords two isomers, where the double bonds of the five-membered ring and the vinyl group adopt trans and cis configurations, respectively (see structures in Figure 2). To identify the lower energy isomer and to aid with the assignment of the observed spectrum, ab initio Hartree−Fock, configuration interaction with single excitations (CIS),[18] complete active space self-consistent field (CASSCF),[19−22] and multireference second-order Rayleigh−Schrödinger perturbation theory (MR-RS2)[23,24] calculations were carried out as well as computations using density functional theory (DFT) and time-dependent DFT (TD-DFT)[25−27] in conjunction with the B3LYP hybrid functional.[28,29] In the higher level CASSCF and subsequent MR-RS2 calculations the geometries were restricted to be of C_s symmetry, i.e., with a planar carbon skeleton. This readily allowed the active space to be chosen to consist of 8 π molecular orbitals (MO), occupied by 8 active electrons (with only two of the 10 π electrons being inactive). The basis sets used are 6-31G(d), 6-311+G(d,p), and 6-311+G(2d,p). TD-B3LYP calculations performed by using the G3Large basis (which is the 6-311+G-(2df,2p) basis extended with a set of p and d core polarization functions on the carbons) yielded nearly identical results to those obtained with the 6-311+G(2d,p) basis. The CASSCF and MR-RS2 calculations were carried out with the MOLPRO 2006.1 programs[30] on the SGI Altix AC computer facility of the Australian Partnership for Advanced Computing at the National Supercomputing Centre, Australian National University, Canberra. The CIS and DFT calculations were performed with the Gaussian03 programs[31] on DEC alpha 600/5/333, COMPAQ XP100/500, and 4-processor Xeon computers of the Theoretical Chemistry group at the University of Sydney.

The cis and trans ground-state equilibrium geometries were computed at the B3LYP/6-31G(d) level of theory, obtaining fully optimized geometries of C_1 symmetry, i.e., with a (slightly) nonplanar carbon (and nonaliphatic hydrogen) skeleton, as well

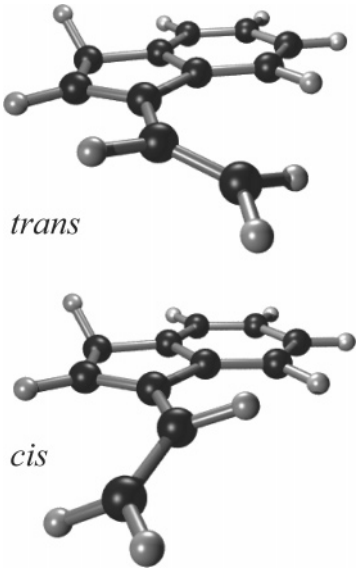

Figure 3. Geometries of local minima on the vinylindene potential energy surface.

as geometries constrained to be of C_s symmetry. As discussed later, the energies of the latter lie only ~100 cm^{-1} higher than their nonplanar counterparts. The actual C_1 structures are illustrated in Figure 3. The torsional (dihedral) angle describing the interconversion of the trans and cis forms is defined for our purposes as being zero in the planar cis form. The local minimum that defines the C_1 cis equilibrium geometry is at a dihedral angle of 29°, while the global minimum, corresponding to the C_1 trans equilibrium geometry has a dihedral angle of 163°. The energy difference between the two C_1 configurations is only ~140 cm^{-1}. Somewhat surprisingly, we were not able to obtain a properly converged result for the S_2 state of the trans isomer with the smallest 6-31G(d) basis.

The geometry of the S_1 state was fully optimized and its harmonic frequencies were calculated at the CIS/6-31G(d) level of theory, for both cis and trans forms. The local minima on the S_1 surface correspond to vinyl torsional angles of 35° (cis) and 145° (trans), respectively, differing from the ground-state angles by 6° and 15°. The resulting zero-point energies of 40 050 and 40 108 cm^{-1} of the cis and trans forms are comparable with those in the ground state, whose values at the HF/6-31G(d) level of theory are 40 912 and 40 967 cm^{-1}, respectively (unscaled values).

Vertical excitation energies were calculated at the MR-RS2, TD-B3LYP, and CIS levels of theory by using basis sets ranging from 6-31G(d) to 6-311+G(d,p) and 6-311+G(2d,p) at the B3LYP/6-31G(d) planar as well as nonplanar geometries. The results are presented in Table 1, along with the corresponding oscillator strengths. Note that in the case of the MR-RS2 calculations the oscillator strengths quoted were obtained at the CASSCF level of theory, which was used to generate the reference states. The common set of CASSCF orbitals for the S_0, S_1, and S_2 states were obtained by a state-averaged calculation with equal weight factors for the three states. In the MR-RS2 calculations, for each state a level shift of 0.2 E_h was used to ensure satisfactory convergence.[32] According to the MR-RS2 calculations the trans isomer is predicted to have higher excitation energies, both to the S_1 and S_2 states. Moreover, the oscillator strength associated with the $S_1 \leftarrow S_0$ transition is predicted to be 2−3 orders of magnitude smaller than that for the $S_2 \leftarrow S_0$ transition.

The oscillator strengths calculated at different basis set quality within the same level of theory are reasonably self-consistent. A notable exception is the $S_1 \leftarrow S_0$ transition calculated at the cis-planar geometry by CASSCF theory (MR-RS2 in Table 1). Here the oscillator strength decreases by a factor of 4 on going from the smallest basis set to the largest. However, these are very small numbers and, if the equilibrium geometry lies near a node on the transition moment surface, the computed oscillator strength will be very sensitive to basis set.

Comparing TD-B3LYP with CASSCF, it is seen that the latter predicts higher oscillator strengths by a factor of between 2 and 5 for the $S_2 \leftarrow S_0$ transition. Similarly, the CIS method at nonplanar geometries also predicts higher *f*-values than TD-B3LYP. The latter is partially due to the higher excitation energies predicted by the CIS method. In general, one should be cautious in calculating an oscillator strength at the equilibrium geometry alone, especially if the transition moment is a strong function of the geometry. For instance, the CASSCF *f*-values for the $S_1 \leftarrow S_0$ transition vary by an order of magnitude between the cis- and trans-planar geometries. For these reasons, the oscillator strength reported in Table 1 should be taken as indicative only. That is, the $S_1 \leftarrow S_0$ transition is much weaker than the $S_2 \leftarrow S_0$ transition, as in benzene, naphthalene, indene, and other aromatic molecules. It should be noted that the CASSCF *f*-values reported here are close to the experimental values reported for indene itself.[34]

The vertical $S_1 \leftarrow S_0$ excitation energies calculated for the planar cis and trans conformers at the highest level of theory (MR-RS2) are 31 113 and 32 090 cm^{-1}, respectively. On the basis of our TD-B3LYP/6-311+G(2d,p) calculations, the effects of nonplanarity on these excitation energies are an increase by 667 cm^{-1} and a decrease by 35 cm^{-1} for the cis and trans forms, respectively. Thus, our best estimates of the vertical $S_1 \leftarrow S_0$ excitation energies are 31 780 and 32 055 cm^{-1}, resulting in a trans−cis difference of just 275 cm^{-1}. The TD-B3LYP and CIS excitation energies are substantially higher than what had been obtained at the MR-RS2 level of theory. Moreover, both the TD-B3LYP and CIS methods predict incorrect ordering of the S_1 and S_2 excited states. This deficiency of these methods, which rely on the excited states being adequately described in terms of singly excited configurations, has been noted by Zilberg et al.[33] in the case of indene itself. Zilberg et al. found the S_1 state of indene to consist largely of an admixture of HOMO → LUMO + 1 and HOMO-1 → LUMO transitions, while the S_2 state was found to arise largely from the HOMO → LUMO transition (see also ref 35). This is also the case for vinylindene. The absence of the appropriate doubly excited configurations from the excited states, especially the S_1 state, is the reason why TD-B3LYP and CIS fail to resolve the correct order among the excited states. Nevertheless, both the TD-B3LYP and the CIS results follow the same trend as the MR-RS2 predictions. In particular, for both S_1 and S_2 states, the trans forms have higher excitation energies than their cis counterparts. Utilizing the computed CIS/6-31G(d) and HF/6-31G(d) zero-point energies (scaled by 0.89) and the TD-B3LYP/6-311+G(2d,p) adiabatic excitation energies, the estimated 0−0 excitation energies are 31 000 and 31 292 cm^{-1} for the cis and trans conformers, respectively, to be compared with our experimental origin of 33 455 cm^{-1}. While not quantitative, we consider such agreement between theory and experiment reasonable, considering the intrinsic difficulties associated with accurate theoretical predictions for a relatively large system such as vinylindene.

Of particular relevance for this study is the comparison of the cis and trans conformers' excitation energies. According to

TABLE 1: Calculated Vertical Electronic Transition Energies and Oscillator Strengths of Vinylindene at Planar and Nonplanar Cis and Trans B3LYP/6-31G(d) Ground-State Geometries

		cis planar				trans planar			
		S_1		S_2		S_1		S_2	
		E (eV)	f	E (eV)	f	E (eV)	f	E (eV)	f
MR-RS2[a]	6-31G(d)	4.27	6.3×10^{-4}	4.96	0.19	4.54	2.9×10^{-3}	NC[b]	
	6-311+G(d,p)	3.92	2.5×10^{-4}	4.54	0.20	4.03	1.1×10^{-3}	4.85	0.22
	6-311+G(2d,p)	3.86	1.7×10^{-4}	4.42	0.19	3.98	1.1×10^{-3}	4.75	0.21
TD-B3LYP	6-31G(d)	4.71	9.7×10^{-3}	4.32	4.2×10^{-2}	4.82	1.1×10^{-2}	4.63	8.2×10^{-2}
	6-311+G(d,p)	4.56	1.2×10^{-2}	4.09	4.1×10^{-2}	4.69	1.5×10^{-2}	4.50	9.9×10^{-2}
	6-311+G(2d,p)	4.55	1.2×10^{-2}	4.07	3.9×10^{-2}	4.68	1.5×10^{-2}	4.48	9.4×10^{-2}
		cis nonplanar				trans nonplanar			
		S_1		S_2		S_1		S_2	
		E (eV)	f	E (eV)	f	E (eV)	f	E (eV)	f
TD-B3LYP	6-31G(d)	4.79	1.1×10^{-2}	4.45	4.3×10^{-2}	4.82	1.3×10^{-2}	4.61	8.0×10^{-2}
	6-311+G(d,p)	4.64	1.7×10^{-2}	4.25	3.9×10^{-2}	4.69	2.0×10^{-2}	4.48	9.3×10^{-2}
	6-311+G(2d,p)	4.63	1.7×10^{-2}	4.23	3.7×10^{-2}	4.67	2.0×10^{-2}	4.46	8.9×10^{-2}
CIS	6-31G(d)	5.91	2.8×10^{-2}	5.35	0.11	5.92	2.1×10^{-2}	5.49	0.19
	6-311+G(d,p)	5.67	4.6×10^{-2}	5.10	0.10	5.69	2.8×10^{-2}	5.29	0.22
	6-311+G(2d,p)	5.62	5.0×10^{-2}	5.07	0.10	5.65	3.4×10^{-2}	5.27	0.21

[a] Oscillator strengths computed at the CASSCF level of theory. [b] No convergence.

the above analysis, the cis form has a marginally lower $S_1 \leftarrow S_0$ excitation energy, by $\sim$300 cm^{-1}. Such a small difference is considered to be well within the theoretical uncertainty associated with our calculations, especially since the deviation of the predicted excitation energies from experiment is approximately an order of magnitude larger. Thus, unfortunately, we cannot identify the conformer(s) giving rise to the observed spectra purely on the basis of quantum chemical computations of their excitation energies. As will be argued below, such identification is possible by the study of the vibrational frequencies.

A relaxed one-dimensional scan of the potential energy surface with respect to the torsional angle was obtained by calculating the B3LYP/6-31G(d) energies at a range of dihedral angles such that at each angle all other geometric parameters were fully optimized. Such scans were also done for the lowest two excited states, S_1 and S_2, at the CIS/6-31G(d) level of theory. The resulting potential energy curves are shown in Figure 4. Qualitatively, they are similar, inasmuch as in all three states the local minima correspond to near planar configurations but the barrier to cis−trans interconversion in the S_2 state, at $\sim$2800 cm^{-1}, is substantially larger than that in the ground ($\sim$1100 cm^{-1}) and S_1 ($\sim$700 cm^{-1}) states. The S_2 state also differs from the other two in that the trans isomer is $\sim$1500 cm^{-1} higher in energy than its cis counterpart. In the ground and S_1 states, for all practical purposes, the energy differences between the two isomers are the same, having been calculated to be less than 100 cm^{-1} different. As the barrier to interconversion between the two minima is on the order of a few k_BT at room temperature, we expect our sample to contain a mixture of the two isomers.

The harmonic frequencies obtained by normal-mode analysis at the two minima are listed in Table 2. Of particular interest in this work are the low-frequency modes. In the ground state, many low-frequency modes involve motions of the vinyl group, with the lowest frequency mode corresponding to torsional motion. The S_0 state of indene itself exhibits a lowest frequency of 188 cm^{-1}, attributed to a skeletal bend.[33] In S_0 trans vinylindene, this mode corresponds to the third lowest frequency (ν_{55}, see Table 2).

Similar to the ground state, the S_1 and S_2 excited states also exhibit many low-frequency modes. In the S_1 state, the lowest frequency mode is the vinyl torsional motion. In the S_2 state the low-frequency modes are not as readily assigned to torsional motion but rather consist of combinations of vinyl motions with skeletal bends and ring puckering.

TABLE 2: Selected Calculated Harmonic Vibrational Frequencies of Vinylindene[a]

	S_0 (B3LYP)		S_1 (CIS)		S_2 (CIS)		
mode	trans	cis	trans	cis	trans	cis	notes
ν_{11}	1649	1643	1655	1661	1637	1597	S_1 Kekulé
ν_{20}	1308	1298	1325	1304	1288	1288	S_0 Kekulé
ν_{22}	1280	1263	1282	1274	1247	1238	S_2 Kekulé
ν_{49}	472	451	420	413	428	444	S_1 ring deform
ν_{50}	430	424	360	352	409	412	S_1 ring deform
ν_{51}	404	403	331	317	366	335	S_1 ring deform
ν_{52}	341	325	300	294	311	320	S_1 ring pucker
ν_{53}	248	239	221	216	195	211	S_1 CH_2, vin. bend
ν_{54}	208	200	172	166	159	168	S_1 vin. i.p. bend
ν_{55}	184	169	150	148	156	151	S_1 skeletal bend
ν_{56}	138	131	111	111	105	109	S_1 indene twist
ν_{57}	69	68	91	69	82	69	S_0, S_1 vin. torsion

[a] B3LYP and CIS frequencies scaled by 0.96 and 0.89, respectively.

V. Discussion

The spectrum presented in Figure 2 exhibits an origin in the vicinity of 4 eV, and Franck−Condon (FC) activity in at least one low-frequency vibrational mode. This is immediately reconcilable with the theoretical prediction of such a transition, with the theory also offering several low-frequency modes for assignment in the LIF spectrum. However, the question remains as to which of the two isomers is responsible for the observed spectrum, or if indeed both isomers are exhibited.

On the basis of the ground-state potential energy curve presented in Figure 4, specifically the similar equilibrium energies and low interconversion barrier, we would expect both isomers to be present in the warmed sample. As described above, the calculated excitation energies are also very close. Generally, the cis excitation energy is calculated to be slightly lower; however, the difference is very small and considered to be within the theoretical uncertainty.

From Table 2 it is seen that the vibrational frequencies of the two isomers are also largely similar. As such, one cannot exclude that the experimental observations arise from one or

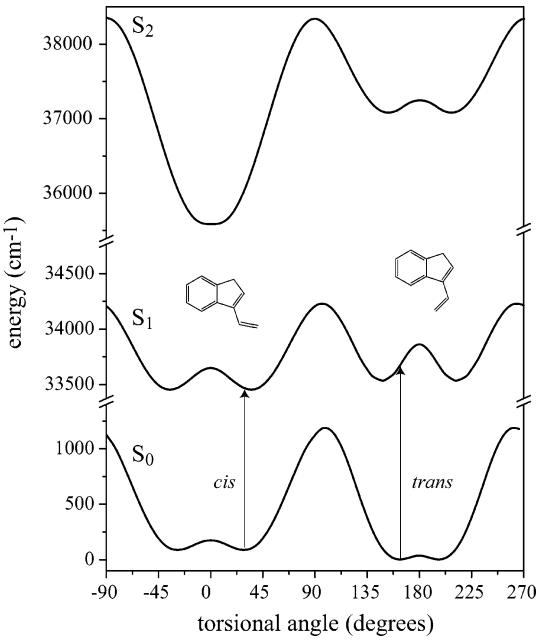

Figure 4. Ground- and excited-state torsional potentials for vinylindene calculated by using DFT and CIS theories (see text). The vertical position of the S_1 state is adjusted to that observed in the LIF spectrum while that of the S_2 state is placed by MR-RS2 theory. Note that the vertical scale for the S_2 state is compressed relative to the other electronic states.

both conformers. The trans isomer is calculated to be slightly lower energy in the ground state: it is only ~100 cm^{-1} lower than the cis form and both might be expected to be present in a room temperature sample.

As a starting point in assigning the observed spectrum we refer to the published R2PI spectrum of indene itself.[34] In the $S_1 \leftarrow S_0$ spectrum of indene reported by Kendler et al., there is virtually no vibrational structure within 350 cm^{-1} of the origin. The first significant vibronic peak, 30_0^1, is placed at 356 cm^{-1}, and corresponds to excitation of a mode described by in-plane counter-rotation of the two rings.[33] This band is observed with an intensity of about 16% of the origin band. The vinylindene counterpart of this band, labeled ν_{51} in Table 2, is calculated to have the slightly lower frequency of 331 cm^{-1} and should be evident in the spectrum. A band displaced 336 cm^{-1} from the origin neatly fits this assignment in terms of both frequency and intensity and is assigned as such in Figure 2. It follows that all structure to lower energy than this band should involve motion of the vinyl group, or of the other conformer to that responsible for the putative origin band.

As illustrated in Figure 4, the equilibrium torsional angle changes only modestly upon electronic excitation in both the trans and cis configurations. As such, some excitation of torsional motion is expected upon making the transition from the S_0 to the S_1 state. The observed, short, 80 cm^{-1} progression is readily assigned to the torsional vibration, ν_{57}, from Table 2. The frequency match for ν_{57} is good, the computed S_1 trans frequency being 91cm^{-1}. If a scaling factor of 0.85 were applied (as Zilberg et al.[33] applied for out-of-plane modes), this match would be even better. However, as Figure 4 reveals, the barrier to "planarity" is low (~300 cm^{-1}) and this motion might not be expected to be harmonic. However, a simple variational one-dimensional calculation based on the potential displayed in Figure 4 predicts that the deviation from harmonicity should remain small for the first few exhibited torsional levels, with a second difference of only about 3 cm^{-1} (the reduced mass was varied to fit the observed position of 57_0^1). Furthermore, a one-dimensional calculation predicts no observable tunneling splittings at our experimental resolution. The simplest assignment based on these considerations is that the 80 cm^{-1} progression observed is due to excitation of the vinyl torsion of the trans conformer, as indicated in Figure 2. One reservation is that the intensity of 57_0^3 is perhaps larger than expected, perhaps indicating an underlying feature.

TABLE 3: Observed Bands of Vinylindene with Assignments[a]

freq (cm^{-1})	assignment	theory[b]
33455 (T_0)	$t0_0^0$	
$T_0 + 80$	$t57_0^1$	91
$T_0 + 161$	$t57_0^2$	
$T_0 + 176$	$t54_0^1$	172
$T_0 + 214$	$t53_0^1$	221
$T_0 + 240$	$t57_0^3$	
$T_0 + 257$	$c0_0^0$	see text
$T_0 + 295$	$t52_0^1$	300
$T_0 + 317$	$c57_0^1$	$c0_0^0$+69
$T_0 + 336$	$t51_0^1$	331
$T_0 + 352$	$t50_0^1$	360
$T_0 + 374$	$c57_0^2$	
$T_0 + 389$	$t49_0^1$	420
$T_0 + 398$		
$T_0 + 415$	$t51_0^1 57_0^1$	
$T_0 + 431$	$t50_0^1 57_0^1$	

[a] See text for detailed discussion. [b] Scaled values from Table 2.

The small features 176 and 214 cm^{-1} from the origin are assigned to ν_{54} and ν_{53} on the basis of the calculated frequency for these vibrations. The lower frequency vibrations, ν_{55} and ν_{56}, are out-of-plane modes of the indenyl moiety and would not be expected to exhibit much Franck−Condon intensity. Modes ν_{54} and ν_{53}, on the other hand, both involve motion of the vinyl moiety, which changes structure between S_0 and S_1. Progressions in ν_{57} should be built onto the 54_1^0 and 53_0^1 transitions, but these progressions are buried under other vibrational bands.

The band observed 257 cm^{-1} from the origin is strong, and if belonging to the same isomer as the origin band, should display the 80 cm^{-1} progression with a similar intensity pattern to that of the origin. However, while there is a peak 79 cm^{-1} to higher energy, its intensity is not consistent with assignment as a progression in ν_{57}. Furthermore, the frequency of 257 cm^{-1} seems too low to be assigned to the next available mode (ν_{52}), which is calculated to be at 300 cm^{-1}. Therefore this band is tentatively ascribed to the other isomer (cis). The CIS calculations suggest that the torsional mode of the cis-isomer should have a frequency 0.75 that of the trans-isomer. Indeed a 60 cm^{-1} progression is observed with a small anharmonicity, consistent with the prediction that the cis-isomer should have a lower barrier to "planarity" than the trans-isomer.

The band appearing 295 cm^{-1} from the origin could be neatly assigned to 52_0^1 but there are several problems with this assignment. The band 79 cm^{-1} to higher energy has an intensity too low to be assigned to the ν_{57} progression and, in any case, this band has already been earmarked as a member of the ν_{57} progression of the cis-isomer. Furthermore, ν_{52} is essentially an out-of-plane mode of the benzene ring, which should not be Franck−Condon strong. Nevertheless, without an alternative, it is assigned in Table 3 to 52_0^1.

The remaining bands have been assigned on the basis of calculated frequencies. The general agreement with the theoretical numbers is satisfactory. However, their assignment should be considered only tentative. It should be noted that the barrier to "planarity" is only about 330 cm^{-1} for the trans geometry and thus the potential energy surface is far from ideally harmonic in this region of the potential. As such, there is likely to be a degree of anharmonic coupling, which will move the observed frequencies and intensities of various vibrational modes away from those expected from simple harmonic considerations.

The assignments discussed above are summarized in Table 3 with the two torsional progressions and some low-frequency assignments illustrated in Figure 2. At this stage many of the assignments remain tentative, mostly a consequence of the uncertainty associated with the presence of two isomers. The matter could be clarified by hole-burning spectroscopy;[12] however, the unstable nature of the compound will undoubtedly make such experiments challenging.

It is of interest to note the predicted large increase in the so-called Kekulé motions of the aromatic ring upon $S_1 \leftarrow S_0$ excitation (Table 2). As explained by Zilberg et al. for indene, this effect may be rationalized in terms of an avoided crossing between the potential curves of the valence bond Kekulé structures. Although it was not possible in the present study to observe this effect directly, Zilberg et al. have shown the CIS method to be effective in resolving the vibrational frequencies of the excited states of indene.[33]

The original motivation of this work was to develop an understanding of the complex chemistry of a benzene discharge. Specifically, we wished to positively identify the mass 142 spectrum obtained by Güthe and co-workers.[13] However, the present spectrum cannot be unambiguously seen in the R2PI spectrum of the benzene discharge. The 3-vinyl-1*H*-indene spectrum overlaps with the congested region of the spectrum of the unidentified species. As such, another carrier must be proposed and its spectrum obtained. While it may be imagined that the current species is formed in a discharge by addition of a linear five-carbon fragment to a cyclic six-carbon species, 2-vinylindene would require either multiple additions to benzene or addition of a branched structure to benzene. The 1-vinylindene should exhibit a chromophore similar to indene itself, which has its origin near 33 600 cm^{-1}—far from the origin of the unidentified mass 142 R2PI spectrum below 32 000 cm^{-1}. As such, it appears unlikely that the mass 142 spectrum is due to any vinylindene (see ref 36).

VI. Conclusions

The laser-induced fluorescence excitation spectrum of 3-vinyl-1*H*-indene has been reported. It exhibits several low-frequency vibrations including a progression in an 80 cm^{-1} mode. From theoretical analysis of the potential energy surfaces in the ground and excited states it was determined that the spectrum observed was likely due to excitation from the energy minimum near the trans arrangement of the double bonds. The 80 cm^{-1} progression is due to torsional motions of the vinyl group. A second torsional progression of 60 cm^{-1} was tentatively assigned to excitation of the cis-isomer. Several other low-frequency modes were tentatively assigned, based on comparison with theoretical calculations.

On the basis of our direct measurement of the LIF spectrum of 3-vinyl-1*H*-indene, we may conclude that the R2PI spectrum of the benzene discharge[4,13] does not contain spectral features which can unambiguously identify the presence of 3-vinyl-1*H*-indene in the discharge. Accordingly, the observed R2PI spectrum associated with mass 142 remains unidentified at the present time. Its identification should provide insight into the carriers of other unidentified spectra produced in the benzene discharge (see ref 36).

Acknowledgment. This research was supported under the Australian Research Council's Discovery funding scheme (project number DP0665831) and the Australian Research Council's Linkage Infrastructure Equipment and Facilities funding scheme (project number LE0560658). P.S. acknowledges the assistance of Dr. P. da Silva and Dr. R. Davey in the synthesis of 3-vinyl-1*H*-indene. We wish to express our thanks to the Australian Partnership for Advanced Computing National Facility for access to the SGI Altix AC system.

References and Notes

(1) Weilmünster, P.; Keller, A.; Homann, K.-H. *Combust. Flame* **1999**, *116*, 62.
(2) Frenklach, M. *Phys. Chem. Chem. Phys.* **2002**, *4*, 2028.
(3) Kim, G. S.; Mebel, A. M.; Lin, S. H. *Chem. Phys. Lett.* **2002**, *361*, 421.
(4) Güthe. F.; Ding, H. B.; Pino, T.; Maier, J. P. *Chem. Phys.* **2001**, *269*, 347.
(5) Snow, T. P.; Witt, A. N. *Science* **1995**, *270*, 1445.
(6) Henning, T.; Salama, F. *Science* **1998**, *282*, 2204.
(7) Herbig, G. H. *Annu. Rev. Astrophys.* **1995**, *33*, 19.
(8) Sarre, P. J. *J. Mol. Spectrosc.* **2006**, *238*, 1.
(9) Ball, C. D.; McCarthy, M. C.; Thaddeus, P. *Astrophys. J.* **2000**, *529*, L61.
(10) Araki, M.; Linnartz, H.; Kolek, P.; Ding, H.; Boguslavskiy, A.; Denisov, A.; Schmidt, T. W.; Motylewski, T.; Cias, P.; Maier, J. P. *Astrophys. J.* **2004**, *616*, 1301.
(11) Reilly, N. J.; Schmidt, T. W.; Kable, S. H. *J. Phys. Chem. A* **2006**, *110*, 12355.
(12) See, for example: Selby, T. M.; Clarkson, J. R.; Mitchell, D.; Fitzpatrick, J. A. J; Lee, H. D.; Pratt, D. W.; Zwier, T. S. *J. Phys. Chem. A* **2005** *109*, 4484. Stearns, J. A.; Zwier, T. S. *J. Phys. Chem. A* **2003**, *107*, 10717. Nguyen, T. V.; Ribblett, J. W.; Pratt, D. W. *Chem. Phys.* **2002**, *283* 279.
(13) Güthe, F. Private communication.
(14) Robinson, A. G.; Winter, P. R.; Zwier, T. S *J. Phys. Chem.* **2002**, *106*, 5789.
(15) Quin, L. D.; Hughes, A. N.; Franklin Lawson, H. H.; Good, A. L. *Tetrahedron* **1983**, *39*, 401.
(16) Chevykalova, M. N.; Ivchenki, P. V.; Nifant'ev, I. E.; Luzikov, Y. N.; Nifant'ev, E. E. *Russ. Chem. Bull. Int. Ed.* **2001**, *50*, 276.
(17) Terentis, A. C.; Stone, M.; Kable, S. H. *J. Phys. Chem.* **1994**, *98*, 10802.
(18) Foresman, J. B.; Head-Gordon, M.; Pople, J. A.; Frisch, M. J. *J. Phys. Chem.* **1992**, *96*, 135.
(19) Roos, B. O.; Taylor, P. R.; Siegbahn, P. E. S. *Chem. Phys.* **1980**, *48*, 157.
(20) Roos, B. O. In *Ab initio Methods in Quantum Chemistry*; Lawley, K. P., Ed.; Wiley: Chichester, U.K., 1987; Vol. II, p 399.
(21) Werner, H.-J.; Knowles, P. J. *J. Chem. Phys.* **1985**, *82*, 5053.
(22) Knowles, P. J.; Werner, H.-J. *Chem. Phys. Lett.* **1985**, *115*, 259.
(23) Werner, H.-J. *Mol. Phys.* **1996**, *89*, 645.
(24) Celani, P.; Werner, H.-J. *J. Chem. Phys.* **2000**, *112*, 5546.
(25) Bauernschmitt, R.; Ahlrichs, R. *Chem. Phys. Lett.* **1996**, *256*, 454.
(26) Stratmann, R. E.; Scuseria, G. E.; Frisch, M. J. *J. Chem. Phys.* **1998**, *109*, 8218.
(27) Casida, M. E.; Jamorski, C.; Casida, K. C.; Salahub, D. R. *J. Chem. Phys.* **1998**, *108*, 4439.
(28) Becke, A. D. *J. Chem. Phys.* **1993**, *98*, 5648.
(29) Lee, C.; Yang, W.; Parr, R. G. *Phys. Rev. B* **1988**, *37*, 785.
(30) Werner, H.-J.; Knowles, P. J.; Lindh, R.; Manby, F. R.; Schütz, M.; Celani, P.; Korona, T.; Rauhut, G.; Amos, R. D.; Bernhardsson, A.; Berning, A.; Cooper, D. L.; Deegan, M. J. O.; Dobbyn, A. J.; Eckert, F.; Hampel C.; Hetzer, G.; Lloyd, A. W.; McNicholas, S. J.; Meyer W.; Mura, M. E.; Nicklass, A.; Palmieri, P.; Pitzer, R.; Schumann, U.; Stoll, H.; Stone, A. J.; Tarroni R.; Thorsteinsson, T. *MOLPRO*, version 2006.1, a package of ab initio programs; see http://www.molpro.net.
(31) Frisch, M. J.; Trucks, G. W.; Schlegel, H. B.; Scuseria, G. E.; Robb, M. A.; Cheeseman, J. R.; Montgomery, J. A., Jr.; Vreven, T.; Kudin, K. N.; Burant, J. C.; Millam, J. M.; Iyengar, S. S.; Tomasi, J.; Barone, V.; Mennucci, B.; Cossi, M.; Scalmani, G.; Rega, N.; Petersson, G. A.;

Nakatsuji, H.; Hada, M.; Ehara, M.; Toyota, K.; Fukuda, R.; Hasegawa, J.; Ishida, M.; Nakajima, T.; Honda, Y.; Kitao, O.; Nakai, H.; Klene, M.; Li, X.; Knox, J. E.; Hratchian, H. P.; Cross, J. B.; Bakken, V.; Adamo, C.; Jaramillo, J.; Gomperts, R.; Stratmann, R. E.; Yazyev, O.; Austin, A. J.; Cammi, R.; Pomelli, C.; Ochterski, J. W.; Ayala, P. Y.; Morokuma, K.; Voth, G. A.; Salvador, P.; Dannenberg, J. J.; Zakrzewski, V. G.; Dapprich, S.; Daniels, A. D.; Strain, M. C.; Farkas, O.; Malick, D. K.; Rabuck, A. D.; Raghavachari, K.; Foresman, J. B.; Ortiz, J. V.; Cui, Q.; Baboul, A. G.; Clifford, S.; Cioslowski, J.; Stefanov, B. B.; Liu, G.; Liashenko, A.; Piskorz, P.; Komaromi, I.; Martin, R. L.; Fox, D. J.; Keith, T.; Al-Laham, M. A.; Peng, C. Y.; Nanayakkara, A.; Challacombe, M.; Gill, P. M. W.; Johnson, B.; Chen, W.; Wong, M. W.; Gonzalez, C.; Pople, J. A. *Gaussian 03*, Revision C.02; Gaussian, Inc.: Wallingford, CT, 2004.

(32) Roos, B. O.; Andersson, S. *Chem. Phys. Lett*. **1995**, *245*, 215.

(33) Zilberg, S.; Kendler, S.; Haas, Y. *J. Phys. Chem.* **1996**, *100*, 10869.

(34) Evleth, E. M. *Theor. Chim. Acta* **1970**, *16*, 22.

(35) Borin, A. C.; Serrano-Andrés, L. *Chem. Phys.* **2000**, *262*, 253.

(36) Newby, J. Private communication. After submission of this paper the 142 carrier was unambiguously identified in Prof. T. S. Zwier's laboratory (Purdue) as a combination of two isomers of phenylcyclopentadiene. One of these isomers has the same Hückel chromophore as 3-vinyl-1*H*-indene.